CrossMark

# Study of Vegetable Biodiesel Enhanced by Gold Nanoparticles Using Thermal-Lens Technique

**J. L. Jiménez-Pérez** · **R. Gutiérrez Fuentes** ·
**Z. N. Correa-Pacheco** · **J. Tánori-Cordova** ·
**A. Cruz-Orea** · **G. López Gamboa**

**Abstract** In this work, experimental results for the enhancement of the thermal diffusivity of a colloidal suspension of gold nanoparticles in biodiesel oil are reported. Different concentrations of Au nanoparticles are prepared using a microemulsion method, by simultaneous reduction of Au ions in the presence of hydrazine as a reducing agent. The thermal diffusivity was found to increase with increasing nanoparticle concentration.

**Keywords** Biodiesel · Gold nanoparticles · Oils ·
Thermal diffusivity · Thermal lens

## 1 Introduction

The cooling of components remains a major technical challenge in many industrial sectors such as transportation, microelectronics, andalternative power generation. As

J. L. Jiménez-Pérez (✉) · Z. N. Correa-Pacheco · G. L. Gamboa
UPIITA-IPN, Avenida Instituto Politécnico Nacional No. 2580, Col. Barrio la Laguna Ticomán,
Gustavo A. Madero, CP 07340 México, DF, México
e-mail: jimenezp@fis.cinvestav.mx

R. G. Fuentes · G. L. Gamboa
Universidad Politécnica del Valle de Toluca (UPVT), km. 5.7, carretera Almolóya de Juárez,
CP 50904 Santiaguito, Tlalcilalcalli, Edo, México

J. Tánori-Cordova
Departamento de Investigación en Polímeros y Materiales, Universidad de Sonora,
A.P. 130, Hermosillo, SON, México

A. Cruz-Orea
Departamento de Física, CINVESTAV-IPN, Av. Instituto Politécnico Nacional 2508 Col. San Pedro
Zacatenco, CP 07360 México, DF, México

a consequence, substantial research is still on-going to enhance the cooling capacity of engineering novel fluids with thermophysical properties superior to the ones of conventional fluids. Since metals have a much higher thermal diffusivity than most fluids, a logical way to try to elevate the thermal diffusivity of fluids is the addition of nanometer-sized metal particles. The use of nanoparticles of different sizes and shapes has been shown to improve heat transfer, and a number of experimental studies on thermal properties of nanofluids have shown a very large enhancement in the thermal conductivity of nanofluids compared to their pure equivalents [1].

In this paper, the thermal diffusivity of vegetable biodiesel containing different concentrations of gold nanoparticles is studied by means of the thermal-lens technique [2].

## 2 Experimental Methods and Materials

Biodiesel, a vegetable oil, consisting of long-chain methyl esters from waste oils, is used in several industrial applications as a key raw material for the production of several commodities such as paints, polymers, lubricants, fuels, etc. Biodiesel oils are a mixture of triglycerides, predominantly derived from an unsaturated and hydroxylated fatty acid, called a ricinoleic acid. In view of studying nanoparticle-induced heat transport enhancement, Au nanoparticles were prepared by the reduction of gold(III) chloride trihydrate using hydrazine as a reducing agent in a microemulsion (reverse micelle) system containing isooctane, deionized water, dioctyl sulfosuccinate sodium salt as a surfactant, and dodecanethiol as a co-surfactant. Next, the Au nanoparticles were mixed into biodiesel, purchased from Biofuels of Mexico (biodiesel C 4), to obtain six sample materials with different concentrations of Au nanoparticles ((1/5, 3/5, 5/5, 7/5, 8/5, and 10/5) mg·mL$^{-1}$).

Measurements of the particle size and morphology were determined by complementary techniques such as transmission electron microscopy (TEM) and UV, respectively. In order to determine the thermal diffusivity of the samples, we have made use of the thermal lens technique.

The TL effect is based on laser-induced heating and time-resolved monitoring on the thermal effects. For a schematic diagram of the used experimental setup, we refer to Ref. [3]. In a step-heating scenario, the time evolution of the probe beam intensity $I(t)$ at the detector is given by Shen et al. [4]

$$I(t) = I(0) \left[ 1 - \frac{\theta}{2} \tan^{-1} \left( \frac{2mV}{\left[(1+2m)^2 + V^2\right] \frac{t_c}{2t} + 1 + 2m + V^2} \right) \right]^2. \quad (1)$$

In Eq. 1, $I(0)$ is the signal intensity when either $t$ or $\theta$ is zero; $\theta$ is proportional to the induced phase shift difference in the probe beam after it passes by the heated area of the sample, and the equation for $\theta$ is [4]

$$\theta = -\frac{P_e A L}{k \lambda_p} \frac{dn}{dT},$$
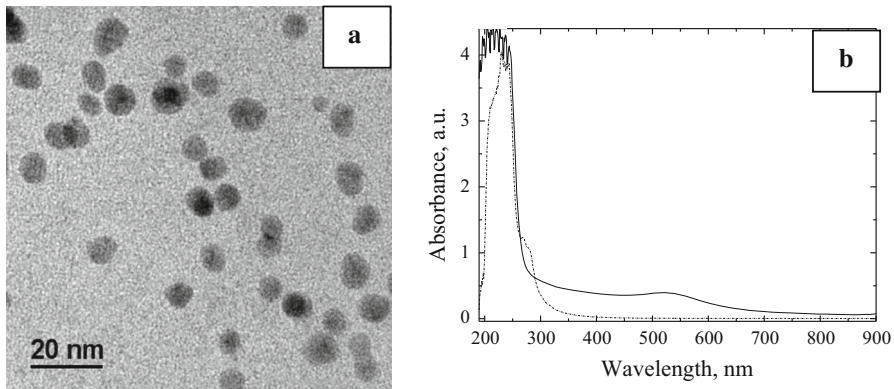
**Fig. 1** (a) Transmission electron microscopy image of the studied gold nanoparticles and (b) absorption spectrum of colloid and biodiesel oil

where $P_e$ (40 mW) is the incident power, $A$ (cm$^{-1}$) is the sample absorption coefficient, $\lambda_p$ (632.8 nm) is the wavelength of the probe beam, $L$ (1 cm) is the cuvette thickness, $k$ (W·m$^{-1}$·K$^{-1}$) is the thermal conductivity, d$n$/d$T$ (K$^{-1}$) is the refractive index temperature coefficient, and $t_c$ is the so-called characteristic time constant of the TL effect's formation. $t_c$ is defined as $t_c = \omega_e^2/4D$ where $\omega_e = (3.98 \pm 0.02) \times 10^{-3}$ cm is the spot size of the excitation laser beam at the sample and $D$ is the thermal diffusivity where $D = k/(\rho c)$ where $k$ is the thermal conductivity, and $\rho$ and $c$ are the density and specific heat, respectively, of the nanofluid. $m = (w_{1p}/w_e)^2$, with $w_{1p}$ (cm) being the probe beam's radius in the sample position and $V = Z_1/Z_c$, with $Z_1$ (cm) being the distance between the minimum beam waist and the sample position and $Z_c = \pi \omega_{op}^2/\lambda_p$, with $\omega_{op}$ (cm) being the minimum probe beam radius; the values of $m$ and $V$ are constants.

Prior to the experiments on the nanofluids, the TL setup was calibrated using distilled water as a sample, resulting in the following values: $m = 22.54 \pm 0.01$ and $V = 0.62 \pm 0.01$.

## 3 Results and Discussion

Figure 1a shows a TEM image of the gold nanoparticles, whose mean diameter was 9 nm. The typical optical absorption spectrum of one of the gold nanoparticle solutions (Fig. 1b) shows an absorption band with a peak at 523 nm. The optical absorption spectrum of biodiesel oil had an absorption band with a peak around 230 nm in the UV region (dotted line).

Figure 2 shows a typical transient thermal-lens signal evolution for biodiesel with an Au nanoparticle concentration of 10/5 mg·mL$^{-1}$. The experimental TL signal is represented by open circles, while the solid line corresponds to the best fit of Eq. 1 to experimental data, leaving $\theta = (7.4 \pm 0.01) \times 10^{-2}$ and $t_c = (17.7 \pm 0.3) \times 10^{-4}$ s as adjustable parameters and $D = (22.6 \pm 0.4) \times 10^{-4}$ cm$^2$·s$^{-1}$ as a best fitting parameter value.
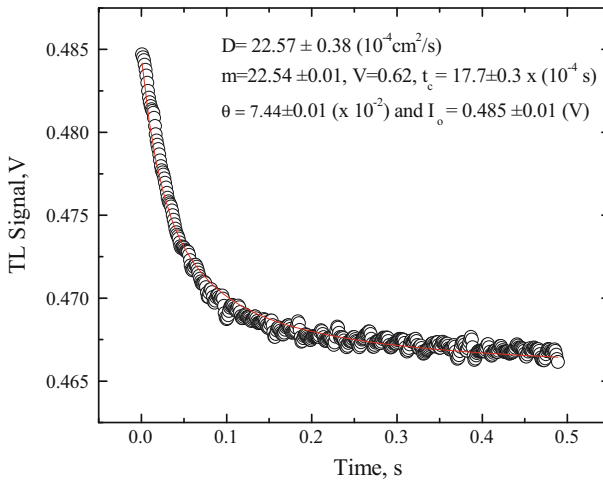
**Fig. 2** Typical transient thermal-lens signal with fitting parameters for biodiesel with concentration of $10/5\,\text{mg}\cdot\text{mL}^{-1}$. Experimental data are depicted as *open circles*. *Solid line* represents the best fit of Eq. 1 to the experimental data

**Table 1** Dependence of the thermal diffusivity and other fitting parameter values of biodiesel nanofluid on the concentration of gold nanoparticles

| Concentration ($\text{mg}\cdot\text{mL}^{-1}$) | $t_c (10^{-4}\,\text{s})$ | $\theta \times 10^{-2}$ | $D\ (10^{-4}\,\text{cm}^2\cdot\text{s}^{-1})$ | $D$ increment (%) |
|---|---|---|---|---|
| Biodiesel (pure) | $23.6 \pm 0.6$ | $4.45 \pm 0.03$ | $17.0 \pm 0.4$ | |
| 1/5 | $22.9 \pm 0.4$ | $9.50 \pm 0.03$ | $17.5 \pm 0.3$ | 3.3 |
| 3/5 | $22.4 \pm 0.4$ | $8.99 \pm 0.04$ | $17.9 \pm 0.3$ | 5.6 |
| 5/5 | $21.4 \pm 0.3$ | $8.33 \pm 0.04$ | $18.7 \pm 0.3$ | 10.6 |
| 7/5 | $20.4 \pm 0.3$ | $8.97 \pm 0.02$ | $19.6 \pm 0.3$ | 15.9 |
| 8/5 | $18.7 \pm 0.3$ | $8.90 \pm 0.03$ | $21.1 \pm 0.3$ | 23.5 |
| 10/5 | $17.7 \pm 0.3$ | $7.44 \pm 0.01$ | $22.6 \pm 0.4$ | 29.4 |

In a similar way, from the best fit of Eq. 1 to the experimental data, the thermal diffusivities of the other nanofluid samples were obtained at room temperature: $D = (17.5 \pm 0.3) \times 10^{-4}\,\text{cm}^2\cdot\text{s}^{-1}$, $D = (17.9 \pm 0.3) \times 10^{-4}\,\text{cm}^2\cdot\text{s}^{-1}$, $D = (18.7 \pm 0.3) \times 10^{-4}\,\text{cm}^2\cdot\text{s}^{-1}$, $D = (19.6 \pm 0.3) \times 10^{-4}\,\text{cm}^2\cdot\text{s}^{-1}$, $D = (21.1 \pm 0.3) \times 10^{-4}\,\text{cm}^2\cdot\text{s}^{-1}$, and $D = (22.6 \pm 0.4) \times 10^{-4}\,\text{cm}^2\cdot\text{s}^{-1}$ for samples with Au nanoparticle concentrations of (1/5, 3/5, 5/5, 7/5, 8/5, and 10/5) $\text{mg}\cdot\text{mL}^{-1}$, respectively. The thermal-diffusivity values obtained for biodiesel with gold nanoparticles are (slightly) higher than that of pure biodiesel, $(16.9 \pm 0.4) \times 10^{-4}\,\text{cm}^2\cdot\text{s}^{-1}$ (the reported value in the literature for pure biodiesel is $14.0 \times 10^{-4}\,\text{cm}^2\cdot\text{s}^{-1}$ [5–8]). The enhancement in the thermal diffusivity goes from 3.3 % to 29.4 % for the different Au nanoparticle concentrations (Table 1). There is a significant increase in the fluid thermal diffusivity with increasing Au nanoparticle concentration.

One possible explanation for the increase in the nanofluid thermal diffusivity can be seen in [9]. Since the Au nanoparticles have an absorption at 523 nm corresponding to a surface plasmon resonance (see Fig. 1b), laser excitation would lead to the generation of phonon scattering at the interface or a transfer of energy from the nanoparticles to the liquid, and also it is expected to depend on the thermal conductivity of the surrounding medium. Related to the heat transfer, since it is a surface phenomenon, its magnitude will increase with an increase in surface area of all the particles. In the case of nanoparticles, the surface area-to-volume ratio is much higher compared to the microparticles. This large total surface area provided by the nanoparticles explains the anomalous increase in the heat transfer rate (or effective thermal conductivity), even when a small volume fraction of nanoparticles is introduced in the liquid medium.

Kumar et al. [10] proposed the following dependence of the rate of heat transfer in dimensionless form $q^*$ for a nanofluid:

$$q^* = \frac{D_{\text{eff}}}{D_{\text{m}}} = c \left( 1 + \frac{k_{\text{p}} \varepsilon r_{\text{m}}}{k_{\text{m}} (1 - \varepsilon) r_{\text{p}}} \right), \tag{2}$$

where $D_{\text{eff}}$ is the effective thermal diffusivity and $D_{\text{m}}$ is the thermal diffusivity of the liquid medium. The enhancement is directly proportional to the ratio of the thermal conductivities ($k_{\text{p}}$ is the thermal conductivity of the nanoparticle material, and $k_{\text{m}}$ is the thermal conductivity of the medium) and to the volume fraction $\varepsilon$ of the nanoparticles (for $\varepsilon \ll 1$), and it is inversely proportional to the radius of the nanoparticles ($r_{\text{m}}$ is the radius of the liquid molecules and $r_{\text{p}}$ is the radius of the nanoparticles), and $C$ is a constant that depends on the ratio of the densities and specific heats of the medium and the nanoparticles.

Figure 3 depicts the dependence of the thermal-diffusivity enhancement as a function of the particle concentration. The dashed line represents the thermal-diffusivity enhancement ratio based on Eq. 2, with $k_{\text{p}} = 380$ W·m$^{-1}$·K$^{-1}$, $k_{\text{m}} = 0.11$ W·m$^{-1}$·K$^{-1}$, $r_{\text{m}} = 15$ nm, and $r_{\text{p}} = 9$ nm.

The model predicts a linear concentration dependence for small concentrations of nanoparticles, which is confirmed for concentrations of (1/5, 3/5, 5/5, and 7/5) mg·mL$^{-1}$. For higher concentration of (8/5 and 10/5) mg·mL$^{-1}$, the experimental increase exceeds the linear dependence for the lower concentrations.

Possibly the disagreement of the experimental values of the model is due to the agglomeration of nanoparticles. In a similar work, Hu et al. [11] reported that AlN nanoparticles with an average diameter of 25 nm were dispersed into ethanol to obtain the desired nanofluids, with castor oil as the selected dispersant. The thermal conductivities of AlN nanofluids were measured by the hot-disk method. Experimental results clearly indicate that the ratios of the thermal conductivities of the AlN suspension increase nonlinearly with the volume fraction. The results are probably based on the relation between the temperature and Brownian motion and agglomeration of nanoparticles. At a low volume fraction, nanoparticles have more intense Brownian motion at not so high temperatures, which can significantly enhance the effective thermal conductivity. They used the theoretical Hamilton and Crosser model for predicting that the thermal conductivity is only dependent on the thermal conductivity of the solid particles and the base liquid and the volume fraction of the solid particles,
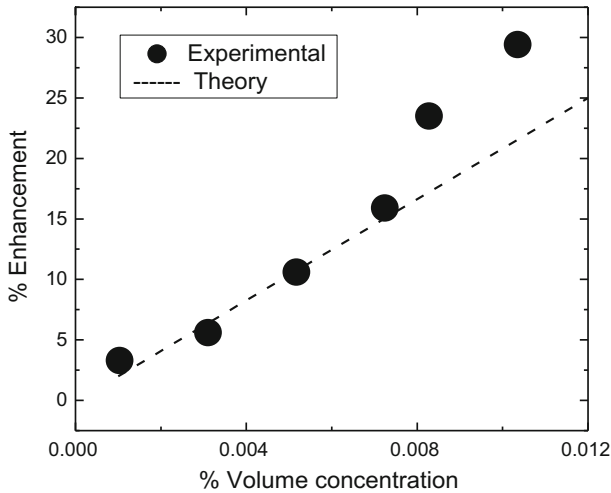
**Fig. 3** Dependence of measured and calculated thermal diffusivities of biodiesel nanofluid on the % volume concentration of Au nanoparticles (with $V = m/\rho$, $\rho_{Au} = 19.32$ g·cm$^{-3}$). *Solid line* represents the best fit of Eq. 1 to the experimental data

and not on the particle size and the interfacial properties. Therefore, comparisons with the experimental data always show that the predictions are linear and lower than the experimental data.

## 4 Conclusions

Experimental results of biodiesel oil samples with Au nanoparticles show an increase in the thermal diffusivity with increasing Au nanoparticle concentration. Heat transport enhancements up to 29 % infer that the use of nanoparticles has significant potential for use in industrial cooling applications. A theoretical model was proposed to describe the dependence of the thermal-diffusivity enhancement as a function of particle concentration. The model predicts a linear concentration dependence for small concentrations of nanoparticles. For higher concentrations, the experimental increase in the thermal-diffusivity ratio exceeds the linear dependence shown at the lower concentrations. Possibly the disagreement of the experimental values with the proposed model is due to agglomeration and the interfacial properties of nanoparticles.

## References

1. S.U.S. Choi, G.Z. Zhang, W. Yu, E.F. Lockwood, A.E. Grulke, Appl. Phys. Lett. **79**, 2252 (2001)
2. S. Bialkowski, *Photothermal Spectroscopy Methods for Chemical Analysis*, vol. 134 in Chemical Analysis (Wiley Inc., New York, 1995)
3. R. Gutiérrez Fuentes, J.F. Sánchez Ramírez, J.L. Jiménez Pérez, J.A. Pescador Rojas, E. Ramón-Gallegos, A. Cruz-Orea, Int. J. Thermophys. **28**, 1048 (2007)

4.  J. Shen, R.D. Lowe, R.D. Snook, Chem. Phys. **165**, 385 (1992)
5.  M. Ventura, E. Simionatto, L.H.C. Andrade, E.L. Simionatto, D. Riva, S.M. Lima, Fuel **103**, 506 (2013)
6.  S.M. Lima, M.S. Figueiredo, L.H.C. Andrade, A.R.L. Caíres, S.L. Oliveira, F. Aristone, Appl. Opt. **48**, 5728 (2009)
7.  R.F. Souza, M.A.R.C. Alencar, C.M. Nascimento, M.G.A. da Silva, M.R. Meneghetti, J.M. Hickmann, Proc. SPIE **6323**, 63231T-1 (2006)
8.  M. Božiková, P. Hlaváč, Acta Technol. Agric. **4**, 90 (2013)
9.  N. Chandrasekharan, P.V. Kamat, J. Hu, G. Jones II, J. Phys. Chem. B **104**, 11103 (2000)
10. D.H. Kumar, H.E. Patel, V.R. Rajeev Kumar, T. Sundarajan, T. Pradeeep, S.K. Das, Phys. Rev. Lett. **93**, 1-144301 (2004)
11. P. Hu, W.L. Shan, F. Yu, Z.S. Chen, Int. J. Thermophys. **29**, 1968 (2008)